418 *Inorg. Chem.* **1988**, *27*, 418-421

Contribution from the Department of Chemistry,
The University of Chicago, Chicago, Illinois 60637

Geometrical-Electronic Relationships in the Series PdP_2, PdPS, and PdS_2

Jeremy K. Burdett* and Barry A. Coddens

Received June 5, 1987

The relationship between electronic and geometrical structure is examined for the series Pd(XY), where XY = P_2, PS, and S_2. Population of high-energy orbitals of the parent three-dimensional PdP_2 structure, antibonding between the nonmetal atoms, leads to a gradual breakup of this arrangement with increasing electron count.

Introduction

Inorganic chemists have always found electron counting a useful approach to organize the shapes associated with the wealth of molecules and solids available to them. An interesting way to relate the structures of series of systems is to follow the geometric response of the structure to the presence of added electrons. Thus[1] in the series $P_4 \rightarrow B_4H_{10} \rightarrow P_4(CF_3)_4 \rightarrow PCl_3$ there is a change in electron count from 20 electrons to 26. Each added pair of electrons results in the breaking of one of the linkages of the parent P_4 tetrahedron. We may understand this[2] in terms of the population of an orbital, antibonding between the atoms of the parent skeleton, which becomes a lone-pair orbital on distortion to the daughter structure (**1**). An analogous series in the solid state is the set of examples ZnS → GaS → GeTe. Here, as the electron count increases from 8 to 10, the three-dimensional framework structure of sphalerite (zinc blende) is converted first into a slab structure and then into a sheet structure (**2**). The building block is a puckered 6^3 sheet of stoichiometry AB (**3**), which can be linked to neighboring sheets above and below. The structures of PdP_2, PdPS, and PdS_2 are geometrically related[3-13] in a similar way. (Some of the selenides and tellurides are also known with similar structures. NiP_2 is isostructural[4] with PdP_2.) Here the building block is a $5^4 + 5^3$ (2:3) sheet (in the Schläfli notation) that contains square-planar Pd atoms (**4**). When the sheets are linked to give the framework structure of PdP_2, a spiral chain of phosphorus atoms running perpendicular to them results (**5**). The phosphorus atoms occur as pairs in the sheets as may be seen in both **4** and **5**. The structure becomes increasingly broken up as the electron count increases from 20 to 22 electrons. (Another way to view the structure of PdS_2 is as a distorted version of the (cubic) pyrite structure, where two of the metal-anion linkages have been elongated to accommodate the Jahn-Teller instability of the low-spin d^8 octahedron.) In this paper we investigate the electronic-structural relationships in this series.

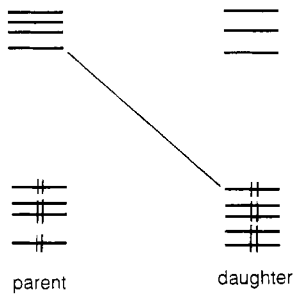

1

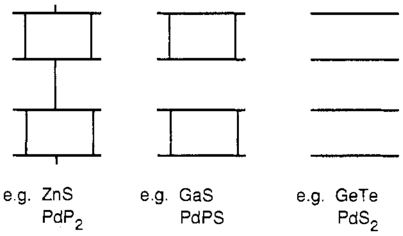

2

3

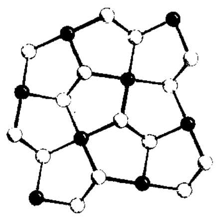

4

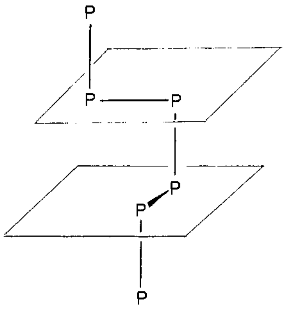

5

Electronic Structure of PdP_2

First we build an electronic description of the parent PdP_2 structure, by using molecular orbital calculations and tight-binding computations based on the extended Hückel method. The parameters are given in the Appendix. We will find it useful to construct the solid from infinite spirals of phosphorus atoms (**5**) linked together by square-planar Pd atoms. The spiral runs roughly perpendicular to the planes so that the P-P linkages alternate in location. Every other linkage lies in the plane of the Pd atoms, leaving the remaining linkages between planes. The structure of PdPS is one where every other intersheet linkage is

---

(1) Mingos, D. M. P. *Nature (London), Phys. Sci.* **1972**, *236*, 99.
(2) See, for example: Burdett, J. K. *Molecular Shapes*; Wiley: New York, 1980.
(3) Zachariasen, W. H. *Acta Crystallogr.* 1963, *16*, 1253.
(4) Rundqvist, S. *Acta Chem. Scand.* **1961**, *15*, 451.
(5) Grønvold, F.; Røst, E. *Acta Crystallogr.* **1957**, *10*, 329.
(6) There is a high-pressure form of PdS_2 that is also a distorted pyrite. Munson, R. A.; Kasper, J. S. *Inorg. Chem.* **1969**, *8*, 1198.
(7) Passaretti, J. D.; Kaner, R. B.; Kershaw, R.; Wold, A. *Inorg. Chem.* **1981**, *20*, 501.
(8) Marzik, J. V.; Kershaw, R.; Dwight, K.; Wold, A. *J. Solid State Chem.* **1982**, *44*, 382.
(9) Bither, T. A.; Donohue, P. C.; Young, H. S. *J. Solid State Chem.* **1971**, *3*, 300.
(10) Grønvold, F.; Røst, E. *Acta Chem. Scand.* **1956**, *10*, 1620.
(11) Jeitschko, W. *Acta Crystallogr., Sect. B.: Struct. Crystallogr. Cryst. Chem.* **1974**, *B30*, 2565.
(12) See, for example: Pearson, W. B. *Crystal Chemistry and Physics of Metals and Alloys*; Wiley: New York, 1972.
(13) See, for example: Burdett, J. K. *Prog. Solid State Chem.* **1984**, *15*, 173. Whangbo, M.-H. In *Crystal Chemistry and Properties of Materials with Quasi-One-Dimensional Structures*; Rouxel, J., Ed.; Reidel: Dordrecht, The Netherlands, 1986.

0020-1669/88/1327-0418$01.50/0 © 1988 American Chemical Society

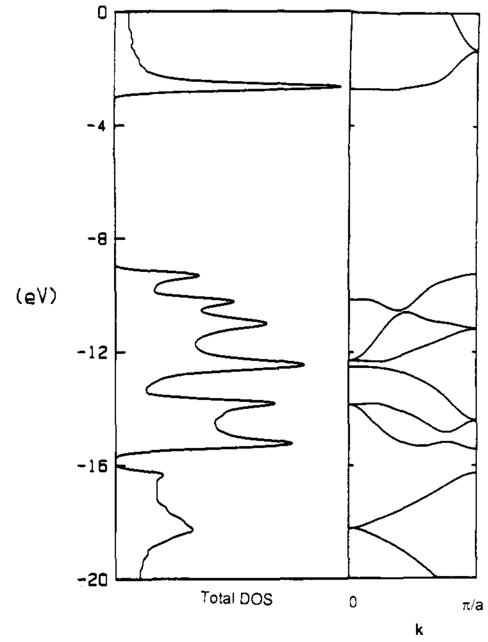

Figure 1. Total density of states (left) and dispersion curve for idealized phosphorus chains with all P–P–P angles 90.0° (right).

broken (giving rise to slabs), and that of PdS$_2$ is one where every intersheet linkage is broken (giving rise to sheets). In PdS$_2$ the remaining S$_2$ dimers lie in the Pd atom plane and comprise the sheet. If the square-planar Pd atom is regarded as Pd^{II}, then the Pd(XY) series may be simply visualized as containing P_2^{2-}, PS^{2-}, and S_2^{2-} units, respectively. P^- is isoelectronic with S, and in the structure of fibrous sulfur[12] and elemental selenium and tellurium, there are infinite spirals of atoms. With extra electrons polysulfide anions are found that contain fragments of such a chain. S_4^{2-}, isoelectronic with PS^{2-}, is a four-atom unit. There are thus close similarities between the structures of the Pd(XY) systems and the structures of smaller units.

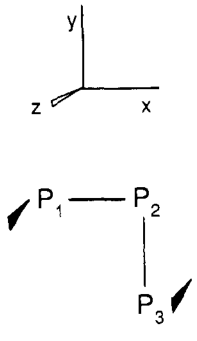

6

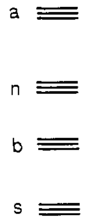

7

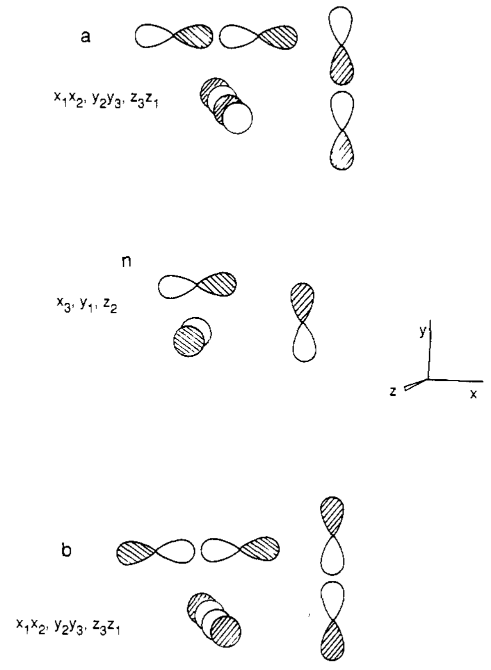

8

We begin by assembling the band structure of the isolated chain. The electronic structure of this unit is very easy to derive. **6** shows the building block of an idealized chain where for didactic simplicity we have set all the P–P–P angles at 90°. First we will ignore π bonding and mixing between the s and p orbitals. A level diagram applicable to all points in the Brillouin zone is shown in **7**. There are simply three bonding levels (b) arising from the p orbitals (x_1x_2, y_2y_3, and z_3z_1) and their corresponding antibonding partners (a). These are localized between pairs of P–P atoms (**8**). Left over are three nonbonding (n) orbitals (x_3, y_1, z_2). Without π interaction between the p orbitals there can be no dispersion associated with any of these bands because the x_1x_2 bonding orbital for example is orthogonal in a σ sense to x_3. When π interactions

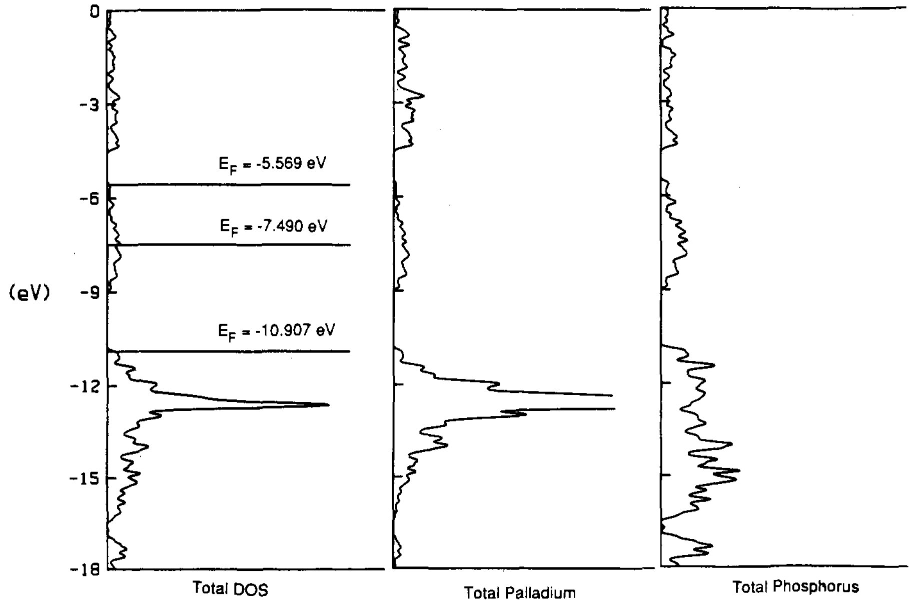

Figure 2. Total electronic density of states for PdP$_2$ (left), projection of total palladium character (middle), and projection of total phosphorus character (top).

Table I. Parameters Used in both Molecular and Solid-State Calculations

orbital		H_{ii}, eV	$\zeta_1{}^a$	$\zeta_2{}^a$	$C_1{}^b$	$C_2{}^b$
Pd	4d	−12.65	5.98	2.613	0.5535	0.6701
	5s	−8.64	2.19			
	5p	−2.68	2.15			
P	3s	−18.60	1.88			
	3p	−12.50	1.63			
	3d	−7.00	1.40			

[a] Slater-type orbital exponents. [b] Coefficients used in double-ζ expansion.

are switched on, these orbitals of the chain may now see each other and these discrete levels broaden into bands. Figure 1 shows both a density of states (DOS) plot and the level dispersion.

There are basically four bands, which are simply derived from the collections of orbitals shown in **7** and **8**. (The bottom of the band derived from the 3s orbitals lies deeper in the diagram and the top of the antibonding band lies off the top.) Notice the large gap between the nonbonding region of the density of states and the antibonding one. The three sets of triplets each break up into a pair and a singlet under the cylindrical symmetry of the orbital problem at the points (0, 0, 0)$2\pi/a$ and (0, 0, 1/2)$2\pi/a$ in the Brillouin zone. Their energetic behavior under the translational symmetry of the problem is relatively straightforward. Easiest to see is that for the collection of phosphorus s orbitals. Since the unit cell is 3 times the simplest one, the basic dispersion behavior of these orbitals is that of a trimerization. Here the bands are folded into three as in **9**. The most bonding level is found at the zone center as a result of the parity of the s orbital.[13] The behavior of the levels b and a are similarly interpreted. The s orbitals and set of σ nonbonding orbitals, n, mix into the orbitals a and b to give directional hybrids. The trimerization process (in this case associated with the 3-fold screw axis along the chain direction) leads to behavior similar to that shown for the s orbitals. Since the s/p hybrid has parity opposite to that of the s orbital, the most bonding level appears at the zone edge for the levels b and the zone center for the levels a. This mixing process is **k**-dependent and serves to distort the shapes of the curves. At the zone center, for example, the totally symmetric combination of x_1x_2, y_2y_3, and z_3z_1 (or its antibonding counterpart) cannot mix with x_3, y_1, or z_2 since the cell-to-cell phase relationships give a zero interaction integral. The behavior of the orbitals n is more complex; their energetic dependence on **k** is controlled by overlap with both a and b.

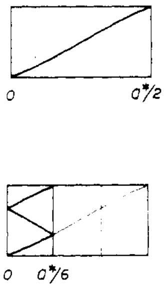

9

For an electronic configuration appropriate to P⁻ or S, all the bonding and nonbonding orbitals are full, and there is formally a single bond between each pair of adjacent atoms in the chain. The electronic description of the real chain in PdP_2 is very similar, even though here the angles are not exactly 90°.

Figure 2 shows our calculated electronic density of states for the PdP_2 structure, with the Fermi levels of the three systems of interest and orbital decompositions, which will be useful in understanding the electronic structure. In Figure 3 we show crystal orbital overlap population (COOP) curves,[14] which describe the bonding or antibonding character between the different pairs of atoms in the structure. Basically the picture is quite simple. The nonmetal chain is so arranged in the structure that the phosphorus atoms use their lone-pair, P–P nonbonding orbitals to coordinate to the metal center. In this metal geometry the dominant interaction of the metal and ligand orbitals in the region of interest is between ligand σ and metal $x^2 - y^2$. The well-known splitting pattern for this geometry is shown in **10**. In the structure of PdP_2 the planes are not exactly flat, and neither do they lie exactly in the xy plane of the crystal; so, in this coordinate system the d orbitals involved in σ interaction with the ligands turn out to be a mixture of $x^2 - y^2$ and yz (Figure 2). Notice that the region between the nonbonding and antibonding levels of the phosphorus chain, which was devoid of energy levels in Figure 1, now contains orbitals that are clearly Pd–P antibonding. They are largely derived from orbitals that are P–P nonbonding, and so we find

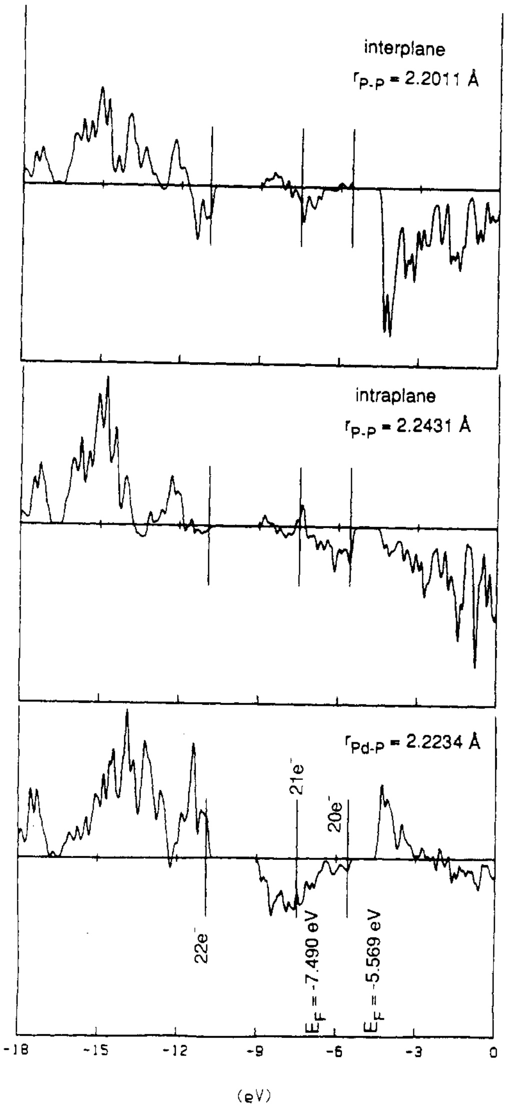

Figure 3. COOP curves for the PdP_2 structure with the Fermi levels for electron counts of 20 (PdP_2), 21 (PdPS), and 22 (PdS_2) per formula unit shown. The bonds represented are the Pd–P bond (bottom), the in-plane P–P bond (middle), and the interplane P–P bond (top).

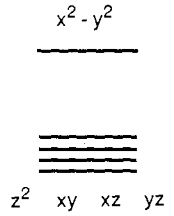

10

---

[14] This visual display of the bonding characteristics was invented by Hoffmann and his co-workers. See, for example: Hoffmann, R. *Angew. Chem.*, in press.

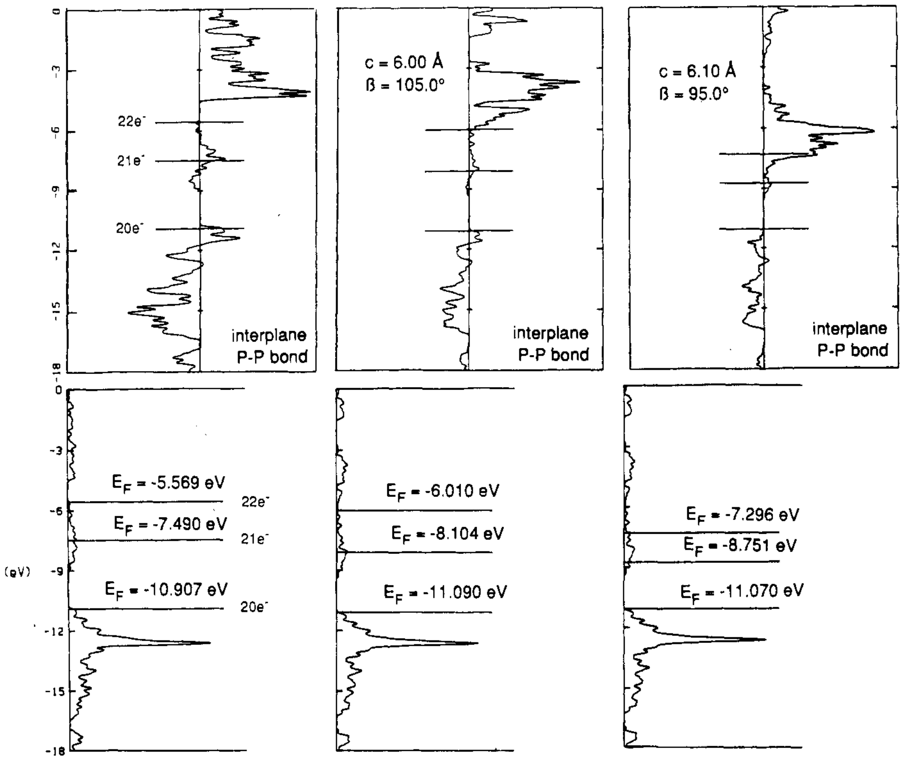

Figure 4. Total density of states and COOP curves of the interplane P–P bond for the distortion of the PdP_2 structure to that of PdPS: (left) undistorted structure; (middle) $c = 6.00$ Å, $\beta = 105.0°$; (right) $c = 6.10$ Å, $\beta = 95.0°$.

in the COOP curves very little P–P bonding or antibonding character in this region, even though the total phosphorus contribution is quite large. It is these orbitals that would be populated for electron counts appropriate to PdPS and PdS_2. The large admixture of Pd d and P p orbitals arises in this system as a result of the energetic proximity of the two sets of atomic orbitals. The building up of the electronic structure is shown schematically in **11**. The calculated band gap for PdP_2 with s and p orbitals only on the phosphorus atoms is 1.92 eV, somewhat different from the observed value of 0.65 eV.[15] We usually find that the numerical value of band gaps using tight-binding theory are better reproduced if d orbitals are added to the phosphorus atoms, and this is true here. The calculated gap becomes 0.70 eV, close to that observed, when they are included.

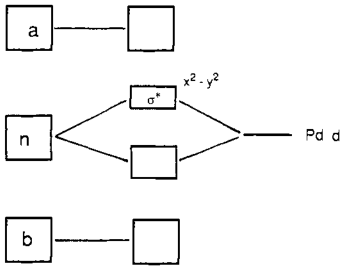

11

Distortion to PdPS and PdS_2

From Figure 3 it is clear to see that, for the PdP_2 structure, the Fermi level for an electron count appropriate for PdPS lies in region that is nonbonding between the anions. Thus the mechanism shown in **1**, population of a low-lying orbital, antibonding between the nonmetal atoms, is an oversimplified picture of the electronic state of affairs. Figure 4 shows how the DOS and also the COOP curves change in character as the distortion from PdP_2 to PdPS proceeds. (This picture was constructed from calculations that used the PdP_2 stoichiometry.) Notice that little change takes place at the Fermi level. It is a higher energy P–P antibonding band that is dropping to lower energy. Eventually it drops below the Pd–P antibonding region and the valence band of the solid with an electron count appropriate to PdPS is a phosphorus lone-pair orbital directed away from the metal at the end of a severed P–P linkage. It is therefore a much higher energy orbital, namely a P–P antibonding one, that plays the key structural role shown in **1**.

We may ask why the structure of PdPS is the broken up one actually observed, rather than something closer to the original PdP_2 structure with an electron located in a Pd–P antibonding, largely metal $x^2 - y^2$ orbital. Square-planar d^9 compounds are after all well-known. AgO, which adopts the tenorite structure, contains square-planar Ag^{II}. This question is a difficult one to answer in general. When does an extra electron become stereochemically active and break bonds, and when does it not? Our one-electron calculations, which in general are very poor at estimating bond energies, are not the place to turn. In the present case a part of the answer must surely lie in the instability of Pd^I relative to that of Pd^{II} and probably in the quite strong Pd–P antibonding nature of the metal $x^2 - y^2$ orbital arising from the interaction shown in **11**.

The picture is quite similar for distortion of the PdPS structure to that of PdS_2. The orbital responsible is again an antibonding orbital, but this time one associated with the four-atom fragment of the slab.

Acknowledgment. This research was supported by the Office of Naval Research.

Appendix

The calculations, both for the molecular fragments and for the solid, were of the extended Hückel type. For the solid a total of 27 **k** points in the irreducible wedge of the Brillouin zone were used to construct the electronic density of states curves for PdP_2 and PdS_2 and 8 for the large cell of PdPS. The parameters are given in Table I. The geometry used was the observed crystal structure for PdP_2, and the distortion of Figure 4 employed a coordinate that connected observed PdP_2 and PdPS structures.

Registry No. PdP_2, 12066-55-6; PdPS, 11083-63-9; PdS_2, 12137-75-6.

---

(15) Hulliger, F. *Nature (London)* **1963**, *200*, 1064.